pISSN 2384-1095
eISSN 2384-1109

iMRI 2021;25:209-217

https://doi.org/10.13104/imri.2021.25.4.209

iMRI
Investigative Magnetic Resonance Imaging

Principles of Magnetic Resonance Angiography Techniques

Taehoon Shin[1,2]

[1]Division of Mechanical and Biomedical Engineering, Ewha Womans University, Seoul, Korea
[2]Graduate Program in Smart Factory, Ewha Womans University, Seoul, Korea

Magnetic resonance angiography (MRA) plays an important role in accurate diagnosis and appropriate treatment planning for patients with arterial disease. Contrast-enhanced (CE) MRA is fast and robust, offering hemodynamic information of arterial flow, but involves the risk of a side effect called nephrogenic systemic fibrosis. Various non-contrast-enhanced (NCE) MRA techniques have been developed by utilizing the fact that arterial blood is moving fast compared to background tissues. NCE MRA is completely free of any safety issues, but has different drawbacks for various approaches. This review article describes basic principles of CE and NCE MRA techniques with a focus on how to generate angiographic image contrast from a pulse sequence perspective. Advantages, pitfalls, and key applications are also discussed for each MRA method.

Keywords: Magnetic resonance angiography; Contrast agent; Non-contrast-enhanced MRA

Review Article

Received: June 16, 2021
Revised: September 11, 2021
Accepted: September 17, 2021

Correspondence to:
Taehoon Shin, Ph.D.
Division of Mechanical and Biomedical Engineering,
Ewha Womans University, 52, Ewhayeodae-gil, Seodaemun-gu,
Seoul 03760, Korea.
Tel. +82-2-3277-4759
Fax. +82-2-3277-3275
E-mail: taehoons@ewha.ac.kr

INTRODUCTION

Depiction of the arterial circulation is essential for appropriate diagnosis and treatment planning of patients with arterial disease. Catheter-based X-ray arteriography has long been the most reliable approach as it offers excellent vessel contrast and spatial resolution as well as short imaging time (1, 2). However, since it is expensive and invasive with the risk of arterial complications (3-5), alternative non-invasive angiography methods have been sought.

Current non-invasive angiography modalities include duplex ultrasound, computerized tomography (CT), and magnetic resonance imaging (MRI). Duplex ultrasound can be used as the first-line diagnostic tool due to its low cost and ability to provide flow information. However, it is highly operator-dependent, and suffers from limited extent of anatomical coverage and obscuration by dense calcification (6, 7). Computerized tomography angiography (CTA) offers superior spatial resolution and high signal-to-noise ratio (SNR), enabling excellent diagnostic sensitivity and specificity (8, 9). However, due to its well-established risks of ionizing radiation and iodinated CT contrast agents, CTA is often been reserved for patients with a high likelihood of pathology (10, 11).

A well-known key advantage of general MRI is that it allows for huge flexibility of tissue contrast. As such, various MR techniques that generate angiographic contrast, i.e., bright arterial signal with dark background signal, have been developed. As different

MRA techniques have their own advantages and drawbacks, the optimal type may differ for specific applications. In this review article, we aim to describe principles of various MRA techniques with a focus on pulse sequences and corresponding image contrast generation mechanisms. Advantages, pitfalls, and key applications are also discussed for each clinically available method as well as experimental ones recently proposed.

Contrast-Enhanced MRA

The most established protocol of MRA uses gadolinium-based contrast agents which shorten T1 of nearby tissues, along with RF spoiled 3D gradient echo sequence (GRE) which achieves pure T1 contrast by nulling transverse magnetization at the end of every TR (12) (Fig. 1). Arterial blood affected by nearby contrast agent will have shorter T1 and experience faster M_z recovery, thus yielding higher signal than tissues not affected by the contrast agent. Typical protocols acquire 3D GRE images prior to administration of contrast agent (pre-contrast). The same 3D acquisitions are then repeated 4-5 times after contrast injection. This time-resolved multi-acquisition strategy can reduce the risk of suboptimal arterial enhancement when imaged too early or the risk of venous contamination when imaged too late (Fig. 2).

Frequency-dependent view sharing, commercially named as TWIST, TRICK, or 4D TRACK depending on MR vendors, is often used to improve temporal resolution of time-resolved CE-MRA (13-15). Based on the fact that most energy of k-space data is concentrated near the origin, this approach updates low-frequency components more often than high-frequency components to improve effective temporal resolution (Fig. 3). Another supplementary approach to improve temporal resolution is application of compressed sensing (16). Images generated by CE-MRA are very sparse (most pixel values are nearly zero) and three-dimensional that are favorable conditions for compressed sensing, thus allowing for high-rate scan acceleration (17-19).

CE MRA is fast and robust, offering hemodynamic information of arterial flow, and has shown excellent diagnostic performance in diverse applications (20-25). However, intravenous administration of contrast agents increases examination costs and patient discomfort, and limits available acquisition time, thus limiting achievable spatial resolution. Furthermore, the risk of nephrogenic systemic fibrosis (NSF) remains an unresolved and potentially devastating clinical issue. While the incidence of NSF has been significantly reduced by screening out

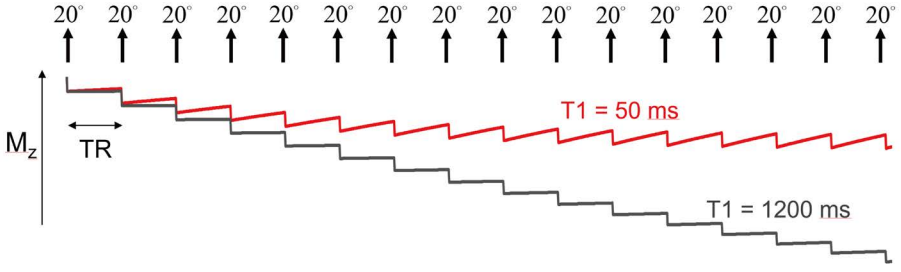

Fig. 1. Simulated longitudinal magnetization (M_z) over excitations in RF-spoiled gradient echo (GRE) imaging with pure T1 weighting.

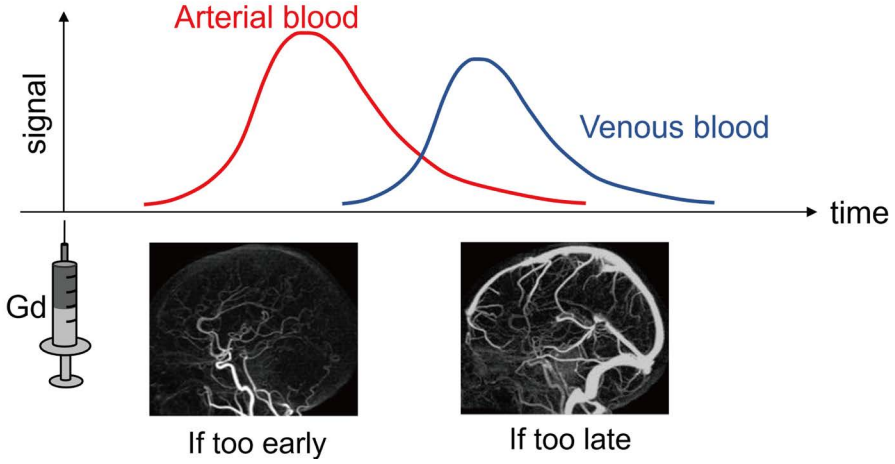

Fig. 2. Time-signal curves for arterial blood and venous blood in gadolinium-based contrast enhanced MR angiography. As the contrast agent flows through the vascular system, arterial blood and venous blood light up sequentially due to increased T1 values by the contrast agent. Image captured too early after the injection of contrast agent may fail to depict distal arteries, while images captured too late may suffer from venous contamination.

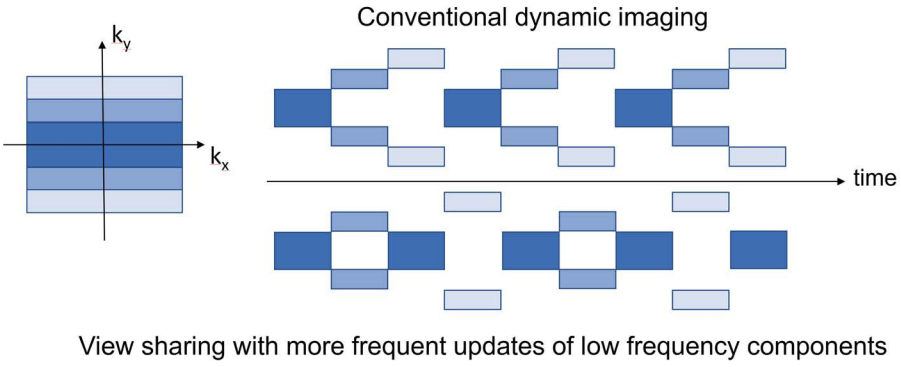

Fig. 3. View sharing strategy with varying update rates for time-resolved dynamic contrast-enhanced MRA. Temporal resolution of dynamic MRA can be improved by updating low frequency components more often than updating high frequency components.

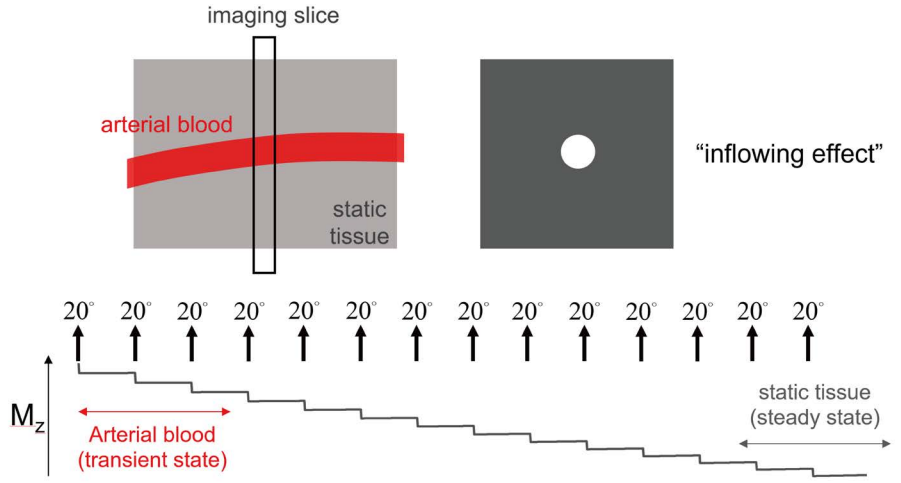

Fig. 4. Principle of time-of-flight (TOF) MRA. When imaging slice is oriented orthogonal to arteries in GRE imaging, static tissues are saturated over repeated readout excitations while arterial blood magnetization remain high in transient state due to exposure to a limited number of excitations.

patients with ≥ stage 4 chronic kidney disease (CKD) and by reducing contrast the dose, the NSF risk continues to be an important safety consideration (26-28).

Time of Flight

Time-of-flight (TOF) imaging is the most classical MRA technique which does not use contrast agents (29, 30). When GRE sequence is applied with imaging slice or slab oriented orthogonal to arterial vessels, the magnetization of stationary tissues can get saturated and reach a steady-state value of small magnitude whereas moving arterial blood experiences only a small number of excitations and retains large magnetization staying in a transient state (Fig. 4). TOF is widely available in clinical practice, and routinely used for neurovascular applications. The major issue in TOF is that in-plane and/or slowly moving arterial blood may experience undesirable large numbers of excitations and therefore result in a signal loss (i.e., deviate from the transient state and get closer to the steady state).

Both 2D and 3D versions of TOF are in active clinical use. 2D TOF is advantageous for the depiction of slow flow due to its thin slice excitation. It is popular for neck angiography. However, achievable resolution in the through-plane direction is limited due to the limitation of minimal possible excitation thickness (~3 mm). On the other hand, 3D TOF enables high spatial resolution in through-plane direction as well. Thus, it is the method of choice for cerebral angiography which requires high resolution in all three directions. As a tradeoff, 3D TOF suffers more from saturation effects than 2D TOF, making it difficult to visualize small vessels with 3D TOF.

Slab-Selective Inversion Recovery

Slab-selective inversion recovery (SS-IR) imaging, commercially named as Inhance inflow IR, B-Trance, or Native, is a non-contrast-enhanced (NCE) technique that is often used for renal and abdominal angiography (31-33). The SS-IR pulse sequence consists of an SS inversion pulse that excites the imaging volume as well as inferior veins, a subsequent delay time, and a segmented 3D acquisition (34, 35) (Fig. 5). When used in abdominal areas, respiratory gating is necessary to mitigate effects of breathing motion.

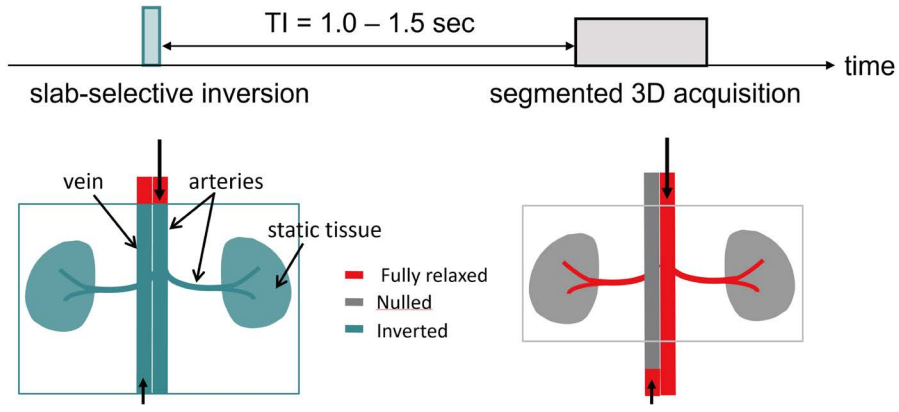

Fig. 5. Principle of slab-selective inversion recovery angiography. The pulse sequence consists of slab-selective inversion, delay time of 1.0-1.5 sec, and segmented 3D acquisition. During the delay time, inverted static tissues and venous blood can only recover partially whereas upstream arterial blood is not affected by the inversion pulse flow into the imaging volume, thereby exhibiting high signals in resultant images.

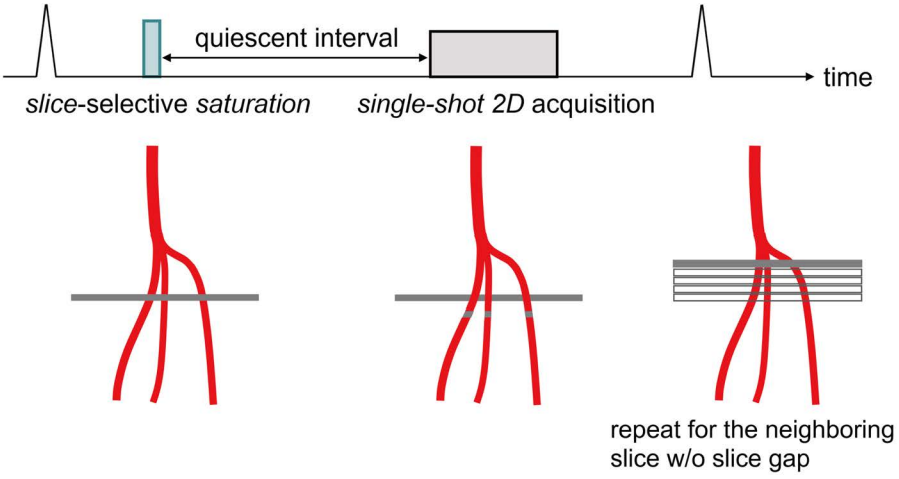

Fig. 6. Principle of quiescent interval single-shot imaging (QISS). The pulse sequence consists of thin saturation preparation, quiescent interval period, and single-shot 2D acquisition. During the quiescent interval, saturated static tissues recover only partially while fresh upstream arterial blood flows into the imaging volume. This is repeated multiple times for neighboring slices without a slice gap to form 3D volume of angiogram.

The inverted static tissues and venous blood are recovered only partially during the inversion delay time, and thus generate small signals. Whereas, fresh upstream arterial blood above the inversion volume is delivered to abdominal aorta and renal arteries, and generates high signal. Since abdominal regions involve breathing motion, respiratory gating should be used for motion-artifact-free images at the cost of increased scan time.

The drawback of SS-IR angiography is that only upstream arterial blood outside the inversion volume contributes to the final angiographic contrast. To ensure sufficient inflow of the upstream arterial blood into the imaging all the way to renal arteries, an inversion delay time of 1.0-1.4 s is commonly used in clinical practice. However, the delay time is longer than the optimal value for suppressing kidney tissues and veins, which is approximately 700 ms at 1.5T, assuming a sufficiently long respiratory cycle for near-complete recovery of magnetization (see Fig. 1b in Ref. (36)). Another consequence of using only upstream arterial blood is limited superior-inferior (S-I) coverage. It would require an impractically long inversion delay time for the upstream arterial blood to reach inferior abdominal aorta and iliac arteries.

Quiescent Interval Single-Shot

Quiescent interval single-shot (QISS) imaging is another inflow-based NCE MRA technique which was initially developed for peripheral applications (7). The QISS pulse sequence consists of a slice-selective saturation pulse that nulls signal of the imaging slice, a subsequent delay time called quiescent interval, and a single-shot 2D acquisition (Fig. 6). This is repeated multiple times for adjacent slice locations without a slice gap to eventually form a 3D angiographic volume. Similar to SS-IR, during the delay time, fresh upstream arterial blood will flow into the imaging slice and appear bright when imaged. Saturated stationary background tissues are recovered only partially, yielding a low signal.

QISS is robust to a wide range of arterial flow patterns due to a short S/I path required for fresh arterial blood to traverse during the saturation delay. Among non-contrast techniques, QISS has shown the greatest promise in patients with peripheral artery disease with advantages of ease of use and short scan (37-39). Since its initial peripheral application, QISS has been used for neck and coronary angiography (40, 41). Limitations of QISS include sub-optimal depiction of slow and in-plane-oriented vessel segments within the saturation region and limited S-I resolution due to limited minimal slice thickness. Thin slab 3D QISS has also been developed recently to overcome the limited S-I resolution (42).

Coronary Angiography

In coronary angiography, the main image contrast should highlight coronary arteries and suppress fat and muscles that closely surround arteries. To enhance arterial signals, segmented 3D acquisition sequence uses balanced steady-state free precession (b-SSFP) or T1 weighted GRE with contrast agents. For muscle and fat suppression, T2 preparation pulse and fat saturation preparation pulse precede the segmented acquisition module.

Due to the need for high-resolution 3D encoding, coronary MRA needs to be performed during free-breathing, which necessitates estimation and correction for respiratory motion. The most established approach applies cylindrical excitation across the diaphragm-air interface followed by 1D spatial encoding in S-I direction (43, 44) (Fig. 7). Resultant 1D signal, when collected over time (cardiac cycles), traces the S-I motion of the diaphragm. Acceptance window (typically 5 mm) is pre-defined so that segmented cardiac data are acquired or abandoned when corresponding diaphragm positions fall within or outside the window. For additional correction for residual respiratory motion (smaller than the gating window), the empirically found correlation between the S-I motion of the diaphragm and the heart is utilized (typically 0.6). Although the diaphragm navigator is in wide clinical use, many studies have found sources of inaccuracy of the diaphragm navigator such as hysteresis during a respiratory cycle and subject-dependent motion correlation between the diaphragm and heart (44-47). In addition, considering S-I motion only might be insufficient for subjects who exhibit significant motions in other directions.

Subtractive Angiography Techniques

Subtractive angiography methods acquire a reference image with bright arterial contrast and another image with black arterial contrast. Subtraction of the reference image by the black artery image will result in artery-only image with suppressed background (Fig. 8a). How to obtain the black artery contrast is the key component, which can be achieved by two approaches: fast spin echo acquisition and diffusion preparation. Half-Fourier fast spin echo (FSE) method utilizes the inherent flow-spoiling of FSE in the readout direction (48). By acquiring two data sets, one at systole and the other at diastole with cardiac gating, spoiled and un-spoiled arterial blood images are obtained (Fig. 8b) and subtracted for background-suppressed artery-only image. Another subtractive NCE MRA method uses a pulse sequence of 90_x-G-180_y-G-90_{-x} as magnetization preparation (termed diffusion preparation or flow sensitive dephasing preparation, Fig. 8c) (49, 50). The magnetization

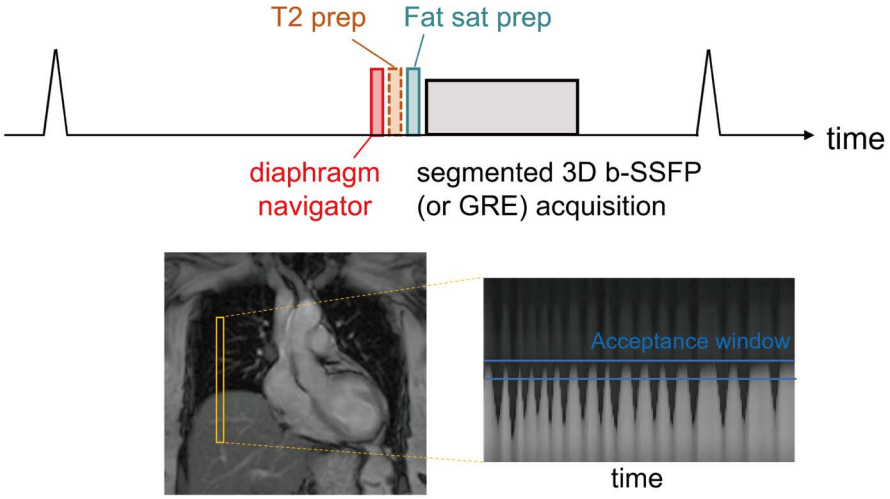

Fig. 7. Principle of free-breathing 3D coronary angiography. The pulse sequence is cardiac gated. It applies respiratory navigator, T2 preparation, fat saturation, and segmented 3D acquisition. The respiratory navigator applies pencil beam-shaped excitation across the liver-air interface to obtain 1D signals over cardiac cycles. It decides whether to record or abandon data segments obtained in the same cardiac cycle based on a pre-defined acceptance window.

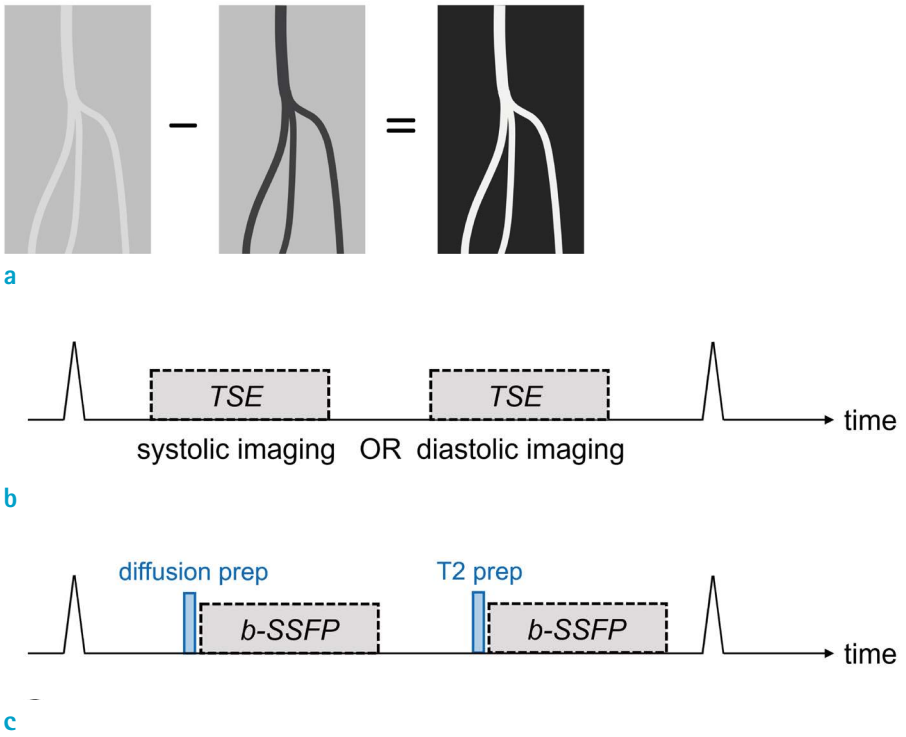

Fig. 8. Principle of subtractive 3D angiography. A reference image with bright arterial contrast is subtracted by another image with a black blood contrast to yield artery-only angiogram (a). One approach acquires reference and black-blood images by employing fast spin echo (FSE) sequence at mid-diastole (where arterial blood flows slowly and looks bright in FSE image) and at systole (where arterial blood looks dark), respectively (b). Another approach acquires black-blood image by applying diffusion preparation and reference image by turning off gradient field in diffusion preparation (c).

response over velocity is sinusoidal for each isochromat. However, due to distribution of varying flow velocities within each voxel, net signal is small for fast moving arterial blood at systole. In this approach, the reference image is obtained by turning off the gradient pulse in the diffusion preparation which is equivalent to T2 preparation.

Subtractive MRA methods can be easily combined with 3D encoding, thus enabling high spatial resolution in all three dimensions. As such, they have shown great promise in lower and upper extremities (51-54). The subtractive nature of this approach enables perfect background suppression and therefore superior artery-to-background contrast. However, it has issues of increased scan time and high sensitivity to motion between acquisitions of two images.

Velocity-Selective Angiography

At the heart of velocity-selective MRA (VS-MRA) is Fourier-based velocity-selective magnetization preparation which generates image contrast by modulating the amplitude and phase of each magnetic spin as an explicit function of its velocity without its regards to spatial location (55, 56). By allocating velocity stop- and pass-bands appropriately, VS preparation can suppress background tissues without perturbing arterial blood, thereby creating angiographic image contrast (Fig. 9). Due to its spatially non-selective nature, VS preparation can be combined with 3D encoding with high spatial resolution and large field of view in all three dimensions, unlike inflow-based 2D multi-slice approaches such as 2D TOF or QISS. VS preparation also generates positive angiographic contrast directly from a single acquisition, as opposed to subtractive 3D approaches that require two acquisitions. With cardiac gating and appropriate trigger delay, a VS preparation pulse is played near the time of peak systolic flow followed by a fat saturation pulse and a 3D segmented data acquisition as in other magnetization prepared imaging. The segmented acquisition module uses b-SSFP at 1.5T and GRE at 3T.

Beginning with peripheral applications, VS-MRA has shown its feasibility for diverse vascular territories, including renal, abdominal, pedal and cerebral arteries (57-61). As VS preparation pulses include many RF and gradient pulses, and therefore prone to B0 and B1 field errors, various versions have been developed to mitigate the effects of field errors (62, 63). Other potential issues include sub-optimal depiction of very slow arterial flow and difficult suppression of fast venous flow.

In conclusion, MRA is available in various types of pulse sequences depending on target arterial territories. CE approaches are the most established ones, offering high angiographic contrast in a time-resolved fashion, but have risk of NSF in patients with reduced kidney function. TOF

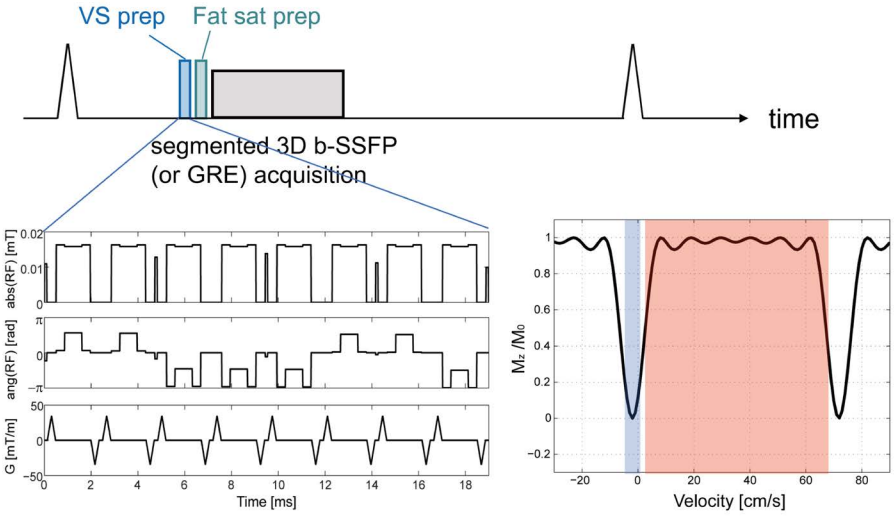

Fig. 9. Velocity-selective magnetization preparation. Velocity-selective excitation pulse sequence consists of a series of hard RF pulses (for excitation) interleaved with unipolar gradients (for velocity encoding) and RF refocusing pulses (left). Simulated Mz profile shows that static and slowly moving tissues are suppressed while fast moving arterial blood is preserved.

MRA is widely used for neurovascular applications without needing contrast agents. Other non-gadolinium-enhanced methods include SS-IR imaging, QISS imaging, respiration-gated imaging, and VS angiography.

Acknowledgments

This work was supported by grants (NRF-2020R1A6A1A03043528, NRF-2020R1A2C1006293) of the Basic Science Research Programs through the National Research Foundation of Korea.

REFERENCES

1. Kadir S. Diagnostic angiography. Philadelphia: Saunders, 1986
2. Abrams HL, Baum S, Pentecost MJ. Abrams' angiograph: vascular and interventional radiology. Boston: Little Brown, 1997
3. Waugh JR, Sacharias N. Arteriographic complications in the DSA era. Radiology 1992;182:243-246
4. Bettmann MA, Heeren T, Greenfield A, Goudey C. Adverse events with radiographic contrast agents: results of the SCVIR Contrast Agent Registry. Radiology 1997;203:611-620
5. Willinsky RA, Taylor SM, TerBrugge K, Farb RI, Tomlinson G, Montanera W. Neurologic complications of cerebral angiography: prospective analysis of 2,899 procedures and review of the literature. Radiology 2003;227:522-528
6. Smith SC Jr, Feldman TE, Hirshfeld JW Jr, et al. ACC/AHA/SCAI 2005 guideline update for percutaneous coronary intervention: a report of the American College of Cardiology/American Heart Association Task Force on Practice Guidelines (ACC/AHA/SCAI Writing Committee to Update the 2001 Guidelines for Percutaneous Coronary Intervention). J Am Coll Cardiol 2006;47:e1-121
7. Edelman RR, Sheehan JJ, Dunkle E, Schindler N, Carr J, Koktzoglou I. Quiescent-interval single-shot unenhanced magnetic resonance angiography of peripheral vascular disease: technical considerations and clinical feasibility. Magn Reson Med 2010;63:951-958
8. Met R, Bipat S, Legemate DA, Reekers JA, Koelemay MJ. Diagnostic performance of computed tomography angiography in peripheral arterial disease: a systematic review and meta-analysis. JAMA 2009;301:415-424
9. Villablanca JP, Jahan R, Hooshi P, et al. Detection and characterization of very small cerebral aneurysms by using 2D and 3D helical CT angiography. AJNR Am J Neuroradiol 2002;23:1187-1198
10. Mehran R, Nikolsky E. Contrast-induced nephropathy: definition, epidemiology, and patients at risk. Kidney Int Suppl 2006:S11-15
11. Rundback JH, Nahl D, Yoo V. Contrast-induced nephropathy. J Vasc Surg 2011;54:575-579
12. Prince MR. Gadolinium-enhanced MR aortography. Radiology 1994;191:155-164
13. van Vaals JJ, Brummer ME, Dixon WT, et al. "Keyhole" method for accelerating imaging of contrast agent uptake. J Magn Reson Imaging 1993;3:671-675
14. Korosec FR, Frayne R, Grist TM, Mistretta CA. Time-resolved contrast-enhanced 3D MR angiography. Magn Reson Med 1996;36:345-351
15. Hennig J, Scheffler K, Laubenberger J, Strecker R. Time-resolved projection angiography after bolus injection of contrast agent. Magn Reson Med 1997;37:341-345

16. Lustig M, Donoho D, Pauly JM. Sparse MRI: the application of compressed sensing for rapid MR imaging. Magn Reson Med 2007;58:1182-1195
17. Rapacchi S, Han F, Natsuaki Y, et al. High spatial and temporal resolution dynamic contrast-enhanced magnetic resonance angiography using compressed sensing with magnitude image subtraction. Magn Reson Med 2014;71:1771-1783
18. Chandarana H, Feng L, Block TK, et al. Free-breathing contrast-enhanced multiphase MRI of the liver using a combination of compressed sensing, parallel imaging, and golden-angle radial sampling. Invest Radiol 2013;48:10-16
19. Jaspan ON, Fleysher R, Lipton ML. Compressed sensing MRI: a review of the clinical literature. Br J Radiol 2015;88:20150487
20. Baum RA, Rutter CM, Sunshine JH, et al. Multicenter trial to evaluate vascular magnetic resonance angiography of the lower extremity. American College of Radiology Rapid Technology Assessment Group. JAMA 1995;274:875-880
21. Gilfeather M, Yoon HC, Siegelman ES, et al. Renal artery stenosis: evaluation with conventional angiography versus gadolinium-enhanced MR angiography. Radiology 1999;210:367-372
22. Liu X, Bi X, Huang J, Jerecic R, Carr J, Li D. Contrast-enhanced whole-heart coronary magnetic resonance angiography at 3.0 T: comparison with steady-state free precession technique at 1.5 T. Invest Radiol 2008;43:663-668
23. Debrey SM, Yu H, Lynch JK, et al. Diagnostic accuracy of magnetic resonance angiography for internal carotid artery disease: a systematic review and meta-analysis. Stroke 2008;39:2237-2248
24. Farb RI, McGregor C, Kim JK, et al. Intracranial arteriovenous malformations: real-time auto-triggered elliptic centric-ordered 3D gadolinium-enhanced MR angiography--initial assessment. Radiology 2001;220:244-251
25. Kruger DG, Riederer SJ, Grimm RC, Rossman PJ. Continuously moving table data acquisition method for long FOV contrast-enhanced MRA and whole-body MRI. Magn Reson Med 2002;47:224-231
26. Kuo PH, Kanal E, Abu-Alfa AK, Cowper SE. Gadolinium-based MR contrast agents and nephrogenic systemic fibrosis. Radiology 2007;242:647-649
27. Martin DR, Krishnamoorthy SK, Kalb B, et al. Decreased incidence of NSF in patients on dialysis after changing gadolinium contrast-enhanced MRI protocols. J Magn Reson Imaging 2010;31:440-446
28. Thomsen HS. NSF: still relevant. J Magn Reson Imaging 2014;40:11-12
29. Masaryk TJ, Laub GA, Modic MT, Ross JS, Haacke EM. Carotid-CNS MR flow imaging. Magn Reson Med 1990;14:308-314
30. Laub GA. Time-of-flight method of MR angiography. Magn Reson Imaging Clin N Am 1995;3:391-398
31. Kanazawa H, Miyazaki M. Time-spatial labeling inversion tag (t-SLIT) using a selective IR-tag on/off pulse in 2D and 3D half-Fourier FSE as arterial spin labeling. In Proceeding of the 10th Annual Meeting ISMRM, 2002:140
32. Braendli M, Bongartz G. Combining two single-shot imaging techniques with slice-selective and non-slice-selective inversion recovery pulses: new strategy for native MR angiography based on the long T1 relaxation time and inflow properties of blood. AJR Am J Roentgenol 2003;180:725-728
33. Katoh M, Buecker A, Stuber M, Gunther RW, Spuentrup E. Free-breathing renal MR angiography with steady-state free-precession (SSFP) and slab-selective spin inversion: initial results. Kidney Int 2004;66:1272-1278
34. Oppelt A, Graumann R, Barfuss H, Fischer H, Hartl W, Shajor W. FISP - a new fast MRI sequence. Electromedica 1986;54:15-18
35. Deshpande VS, Shea SM, Laub G, Simonetti OP, Finn JP, Li D. 3D magnetization-prepared true-FISP: a new technique for imaging coronary arteries. Magn Reson Med 2001;46:494-502
36. Atanasova IP, Kim D, Lim RP, et al. Noncontrast MR angiography for comprehensive assessment of abdominopelvic arteries using quadruple inversion-recovery preconditioning and 3D balanced steady-state free precession imaging. J Magn Reson Imaging 2011;33:1430-1439
37. Hodnett PA, Koktzoglou I, Davarpanah AH, et al. Evaluation of peripheral arterial disease with nonenhanced quiescent-interval single-shot MR angiography. Radiology 2011;260:282-293
38. Ward EV, Galizia MS, Usman A, Popescu AR, Dunkle E, Edelman RR. Comparison of quiescent inflow single-shot and native space for nonenhanced peripheral MR angiography. J Magn Reson Imaging 2013;38:1531-1538
39. Wu G, Yang J, Zhang T, et al. The diagnostic value of non-contrast enhanced quiescent interval single shot (QISS) magnetic resonance angiography at 3T for lower extremity peripheral arterial disease, in comparison to CT angiography. J Cardiovasc Magn Reson 2016;18:71
40. Koktzoglou I, Aherne EA, Walker MT, Meyer JR, Edelman RR. Ungated nonenhanced radial quiescent interval slice-selective (QISS) magnetic resonance angiography of the neck: evaluation of image quality. J Magn Reson Imaging 2019;50:1798-1807

41. Edelman RR, Giri S, Pursnani A, Botelho MP, Li W, Koktzoglou I. Breath-hold imaging of the coronary arteries using Quiescent-Interval Slice-Selective (QISS) magnetic resonance angiography: pilot study at 1.5 Tesla and 3 Tesla. J Cardiovasc Magn Reson 2015;17:101
42. Koktzoglou I, Huang R, Ong AL, Aouad PJ, Walker MT, Edelman RR. High spatial resolution whole-neck MR angiography using thin-slab stack-of-stars quiescent interval slice-selective acquisition. Magn Reson Med 2020;84:3316-3324
43. Wang Y, Riederer SJ, Ehman RL. Respiratory motion of the heart: kinematics and the implications for the spatial resolution in coronary imaging. Magn Reson Med 1995;33:713-719
44. Danias PG, Stuber M, Botnar RM, Kissinger KV, Edelman RR, Manning WJ. Relationship between motion of coronary arteries and diaphragm during free breathing: lessons from real-time MR imaging. AJR Am J Roentgenol 1999;172:1061-1065
45. Nehrke K, Bornert P, Manke D, Bock JC. Free-breathing cardiac MR imaging: study of implications of respiratory motion--initial results. Radiology 2001;220:810-815
46. Taylor AM, Keegan J, Jhooti P, Firmin DN, Pennell DJ. Calculation of a subject-specific adaptive motion-correction factor for improved real-time navigator echo-gated magnetic resonance coronary angiography. J Cardiovasc Magn Reson 1999;1:131-138
47. Keegan J, Gatehouse P, Yang GZ, Firmin D. Coronary artery motion with the respiratory cycle during breath-holding and free-breathing: implications for slice-followed coronary artery imaging. Magn Reson Med 2002;47:476-481
48. Miyazaki M, Sugiura S, Tateishi F, Wada H, Kassai Y, Abe H. Non-contrast-enhanced MR angiography using 3D ECG-synchronized half-Fourier fast spin echo. J Magn Reson Imaging 2000;12:776-783
49. Fan Z, Sheehan J, Bi X, Liu X, Carr J, Li D. 3D noncontrast MR angiography of the distal lower extremities using flow-sensitive dephasing (FSD)-prepared balanced SSFP. Magn Reson Med 2009;62:1523-1532
50. Priest AN, Graves MJ, Lomas DJ. Non-contrast-enhanced vascular magnetic resonance imaging using flow-dependent preparation with subtraction. Magn Reson Med 2012;67:628-637
51. Priest AN, Joubert I, Winterbottom AP, See TC, Graves MJ, Lomas DJ. Initial clinical evaluation of a non-contrast-enhanced MR angiography method in the distal lower extremities. Magn Reson Med 2013;70:1644-1652
52. Lim RP, Fan Z, Chatterji M, et al. Comparison of nonenhanced MR angiographic subtraction techniques for infragenual arteries at 1.5 T: a preliminary study. Radiology 2013;267:293-304
53. Liu X, Fan Z, Zhang N, et al. Unenhanced MR angiography of the foot: initial experience of using flow-sensitive dephasing-prepared steady-state free precession in patients with diabetes. Radiology 2014;272:885-894
54. Sheehan JJ, Fan Z, Davarpanah AH, et al. Nonenhanced MR angiography of the hand with flow-sensitive dephasing-prepared balanced SSFP sequence: initial experience with systemic sclerosis. Radiology 2011;259:248-256
55. de Rochefort L, Maitre X, Bittoun J, Durand E. Velocity-selective RF pulses in MRI. Magn Reson Med 2006;55:171-176
56. Shin T, Worters PW, Hu BS, Nishimura DG. Non-contrast-enhanced renal and abdominal MR angiography using velocity-selective inversion preparation. Magn Reson Med 2013;69:1268-1275
57. Shin T, Hu BS, Nishimura DG. Off-resonance-robust velocity-selective magnetization preparation for non-contrast-enhanced peripheral MR angiography. Magn Reson Med 2013;70:1229-1240
58. Qin Q, Shin T, Schar M, Guo H, Chen H, Qiao Y. Velocity-selective magnetization-prepared non-contrast-enhanced cerebral MR angiography at 3 Tesla: improved immunity to B0/B1 inhomogeneity. Magn Reson Med 2016;75:1232-1241
59. Watson JDB, Grasu B, Menon R, Pensy R, Crawford RS, Shin T. Novel, non-gadolinium-enhanced magnetic resonance imaging technique of pedal artery aneurysms. J Vasc Surg Cases Innov Tech 2017;3:87-89
60. Shin T, Menon RG, Thomas RB, et al. Unenhanced velocity-selective MR angiography (VS-MRA): initial clinical evaluation in patients with peripheral artery disease. J Magn Reson Imaging 2019;49:744-751
61. Zhu D, Li W, Liu D, et al. Non-contrast-enhanced abdominal MRA at 3 T using velocity-selective pulse trains. Magn Reson Med 2020;84:1173-1183
62. Shin T, Qin Q, Park JY, Crawford RS, Rajagopalan S. Identification and reduction of image artifacts in non-contrast-enhanced velocity-selective peripheral angiography at 3T. Magn Reson Med 2016;76:466-477
63. Shin T, Qin Q. Characterization and suppression of stripe artifact in velocity-selective magnetization-prepared unenhanced MR angiography. Magn Reson Med 2018;80:1997-2005